Top quark forward-backward asymmetry and charge asymmetry in left-right twin Higgs model

Lei Wang[1], Lei Wu[2], Jin Min Yang[2]

[1] *Department of Physics, Yantai University, Yantai 264005, China*

[2] *State Key Laboratory of Theoretical Physics,*

Institute of Theoretical Physics, Academia Sinica, Beijing 100190, China

Abstract

In order to explain the Tevatron anomaly of the top quark forward-backward asymmetry A^t_{FB} in the left-right twin Higgs model, we choose to give up the lightest neutral particle of $\hat{h}$ field as a stable dark matter candidate. Then a new Yukawa interaction for $\hat{h}$ is allowed, which can be free from the constraint of same-sign top pair production and contribute sizably to A^t_{FB}. Considering the constraints from the production rates of the top pair ($t\bar{t}$), the top decay rates and $t\bar{t}$ invariant mass distribution, we find that this model with such new Yukawa interaction can explain A^t_{FB} measured at the Tevatron while satisfying the charge asymmetry A^t_C measured at the LHC. Moreover, this model predicts a strongly correlation between A^t_C at the LHC and A^t_{FB} at the Tevatron, i.e., A^t_C increases as A^t_{FB} increases.

PACS numbers: 14.65.Ha,12.60.Fr,14.80.Ec,14.80.Fd

I. INTRODUCTION

The forward-backward asymmetry A^t_{FB} in top quark pair production has been measured by the two experimental groups at the Tevatron. The CDF measured the asymmetry in the $\ell + j$ channel and obtained $A^t_{FB}(CDF) = 0.158 \pm 0.074$ [1], which is nearly consistent with the D0 result $A^t_{FB}(D0) = 0.19 \pm 0.065$ [2]. These results exceed SM prediction, $A^t_{FB}(SM) = 0.058 \pm 0.009$, which arises from NLO QCD diagrams [3]. Including the resummation of soft-gluon emission at NNLL, Ref. [4] gives the currently most precise QCD prediction, $0.072^{+0.011}_{-0.007}$. The CDF also reported an abnormally large value of A^t_{FB} for $m_{t\bar{t}} > 450$ GeV [1], which, however, is not confirmed by D0 collaboration [2].

To explain A^t_{FB}, various attempts have been tried, such as via the s-channel exchange of an axi-gluon [5] or the t-channel exchange of Z', W' and a scalar [6–12] or through an effective model-independent way [13, 14]. In this work we will try to explain A^t_{FB} in the framework of the left-right twin Higgs model (LRTH) [15–17]. In this model, a discrete left-right symmetry ensures the absence of one-loop quadratic divergence of the SM Higgs mass, which emerges as a pseudo-Goldstone boson once a global symmetry is spontaneously broken. The resulting Higgs boson mass is naturally around the electroweak scale when the cut-off scale of the theory is around 5-10 TeV. In the original LRTH, the lightest neutral particle of $\hat{h}$ field is stable and thus can be a candidate for weakly interacting massive particle (WIMP) dark matter [18]. We found that the original LRTH does not contribute to A^t_{FB} sizably, so we choose to give up the dark matter candidate. Then a new Yukawa interaction for $\hat{h}$ is allowed, which is found to contribute sizably to A^t_{FB}.

In our analysis we will consider the following observables:

(1) A^t_{FB} in the $t\bar{t}$ rest frame at Tevatron, which is defined by [10]

$$A^t_{FB} = A^{NP}_{FB} \times R + A^{SM}_{FB} \times (1 - R) \tag{1}$$

where $A^{SM}_{FB} = 0.058$ is the asymmetry in the SM, and

$$A^{NP}_{FB} = \frac{\sigma^{NP}(\Delta y > 0) - \sigma^{NP}(\Delta y < 0)}{\sigma^{NP}(\Delta y > 0) + \sigma^{NP}(\Delta y < 0)}, \tag{2}$$

$$R = \frac{\sigma^{NP}}{\sigma^{SM} + \sigma^{NP}} \tag{3}$$

are the asymmetry induced by the new physics and the fraction of the new physics

contribution to the total cross section, respectively. Δy is the rapidity difference between a top and an anti-top.

(2) The charge asymmetry of $t\bar{t}$ production at LHC, defined by

$$A_C^t = A_C^{NP} \times R + A_C^{SM} \times (1 - R) \tag{4}$$

where $A_{FB}^{SM} = 0.013$ is the asymmetry in the SM [20], and

$$A_C^{NP} \equiv \frac{\sigma^{NP}(|\eta_t| > |\eta_{\bar{t}}|) - \sigma^{NP}(|\eta_t| < |\eta_{\bar{t}}|)}{\sigma^{NP}(|\eta_t| > |\eta_{\bar{t}}|) + \sigma^{NP}(|\eta_t| < |\eta_{\bar{t}}|)}, \tag{5}$$

$$R = \frac{\sigma^{NP}}{\sigma^{SM} + \sigma^{NP}} \tag{6}$$

are the asymmetry induced by the new physics and the fraction of the new physics contribution to the total cross section, respectively. η_t and $\eta_{\bar{t}}$ are respectively the pseudo-rapidity of top and anti-top quark in the laboratory frame. This asymmetry reflects that the top quarks on average are more boosted than the anti-top quarks, which is sensitive to new physics beyond the SM [14, 19]. The CMS collaboration has recently measured the quantity with an integrated luminosity of 1.09 fb^{-1} and obtained $A_C^t = -0.016 \pm 0.030^{+0.010}_{-0.019}$, which is consistent with the SM prediction [20]. The uncertainties of the ATLAS measurement of the charge asymmetry are of similar size with respect to the CMS result [21].

(3) The $t\bar{t}$ total production cross sections at Tevatron and LHC. The current cross section measured at Tevatron is $\sigma^{exp} = 7.50 \pm 0.48$ pb for $m_t = 172.5$ GeV [22], while the SM cross section is $\sigma^{SM} = 7.46^{+0.66}_{-0.80}$ pb from [23] and $\sigma^{SM} = 6.30 \pm 0.19^{+0.31}_{-0.23}$ pb from [24]. The $t\bar{t}$ total production cross section measured recently at LHC with the center of mass energy 7 TeV is $\sigma^{exp} = 176 \pm 5^{+13}_{-10} \pm 7$ pb from ATLAS [25] and $\sigma^{exp} = 168 \pm 18 \pm 14 \pm 7$ pb from CMS [26], while the SM cross section is $\sigma^{SM} = 165.80^{+4.44}_{-6.99} \pm 9.10 \pm 11.6$ pb from [23] and $\sigma^{SM} = 157.92^{+7.79}_{-8.88} \pm 8.67 \pm 11.9$ pb from [27]. Here, we conservatively require $-0.12 < \frac{\sigma^{NP}}{\sigma^{SM}} < 0.3$ for the Tevatron and $-0.25 < \frac{\sigma^{NP}}{\sigma^{SM}} < 0.25$ for the LHC.

(4) The top quark can decay into a light quark and a scalar particle for the scalar mass is light enough. The measurement of the total top width is $\Gamma_t^{exp} = 1.99^{+0.69}_{-0.55}$ GeV [28], and is in agreement with the SM value $\Gamma_t^{SM} = 1.3$ GeV, which sets a limit on the partial width of any new decay mode.

Finally, we will discuss the constraints from the experimental data of $t\bar{t}$ invariant mass distribution and single top quark production.

This work is organized as follows. In Sec. II, we briefly review the left-right twin Higgs model and then introduce a new Yukawa interaction for $\hat{h}$. In Sec. III, we study the top quark observables mentioned above, and focus on the top quark forward-backward asymmetry at Tevatron and charge asymmetry at LHC under the constraints of the other observables. Finally, we give our conclusion in Sec. IV.

II. LRTH MODEL WITH NEW YUKAWA INTERACTION

The LRTH model [16, 17] has a global symmetry $U(4) \times U(4)$ with a gauged $SU(2)_L \times SU(2)_R \times U(1)_{B-L}$ subgroup. The twin symmetry is identified as a left-right symmetry with interchanging L and R, which implies that the gauge couplings of $SU(2)_L$ and $SU(2)_R$ are identical ($g_{2L} = g_{2R} = g_2$).

A pair of Higgs fields, H and $\hat{H}$, are introduced, which transform as $(\mathbf{4}, \mathbf{1})$ and $(\mathbf{1}, \mathbf{4})$ respectively under the global symmetry. They can be written as

$$H = \begin{pmatrix} H_L \\ H_R \end{pmatrix}, \qquad \hat{H} = \begin{pmatrix} \hat{H}_L \\ \hat{H}_R \end{pmatrix}, \tag{7}$$

where $H_{L,R}$ and $\hat{H}_{L,R}$ are two component objects which are charged under $SU(2)_L \times SU(2)_R \times U(1)_{B-L}$ as

$$H_L \text{ and } \hat{H}_L : (\mathbf{2}, \mathbf{1}, 1); \quad H_R \text{ and } \hat{H}_R : (\mathbf{1}, \mathbf{2}, 1). \tag{8}$$

The SM-like Higgs doublet $h = (h^+, h^0)^T$ and the new doublet $\hat{h} = (\hat{h}^+, \hat{h}^0)^T$ reside in H_L and $\hat{H}_L$, respectively.

Each Higgs acquires a non-zero VEV as

$$< H > \; = \; (\; 0 \;\; 0 \;\; 0 \;\; f \;)^T, \qquad < \hat{H} > \; = \; (\; 0 \;\; 0 \;\; 0 \;\; \hat{f} \;)^T, \tag{9}$$

which breaks one of the $U(4)$ to $U(3)$ and yields seven Nambu-Goldstone bosons. The gauge symmetry $SU(2)_L \times SU(2)_R \times U(1)_{B-L}$ is broken down to $U(1)_{EM}$, and six out of the fourteen Goldstone bosons are respectively eaten by the SM gauge bosons W and Z, and additional gauge boson W_H and Z_H with masses of a few TeV. In addition to the SM-like Higgs, we are left with the two neutral pseudoscalar ϕ^0 and $\hat{A}$, one neutral scalar $\hat{S}$, and the charged scalar $\phi^{\pm}$ and $\hat{h}^{\pm}$. Here $\hat{S}$ and $\hat{A}$ are from $\hat{h}^0 = (\hat{S} + i\hat{A})/\sqrt{2}$.

The SM quarks and leptons are charged under $SU(2)_L \times SU(2)_R \times U(1)_{B-L}$ as

$$L_{L\alpha} = -i \begin{pmatrix} \nu_{L\alpha} \\ l_{L\alpha} \end{pmatrix} : (\mathbf{2}, \mathbf{1}, -1), \qquad L_{R\alpha} = \begin{pmatrix} \nu_{R\alpha} \\ l_{R\alpha} \end{pmatrix} : (\mathbf{1}, \mathbf{2}, -1),$$
$$Q_{L\alpha} = -i \begin{pmatrix} u_{L\alpha} \\ d_{L\alpha} \end{pmatrix} : (\mathbf{2}, \mathbf{1}, 1/3), \qquad Q_{R\alpha} = \begin{pmatrix} u_{R\alpha} \\ d_{R\alpha} \end{pmatrix} : (\mathbf{1}, \mathbf{2}, 1/3) \tag{10}$$

with α being the family index.

After the doublet h residing in H_L acquires the VEV, $v \approx 246$ GeV, the masses of the first two generation quarks and bottom quark can be obtained from [17]

$$\mathcal{L}_Y = \frac{\lambda_u^{\alpha\beta}}{\Lambda}(\bar{Q}_{L\alpha}\tau_2 H_L^*)(H_R^T \tau_2 Q_{R\beta}) + \frac{\lambda_d^{\alpha\beta}}{\Lambda}(\bar{Q}_{L\alpha} H_L)(H_R^\dagger Q_{R\beta}) + h.c., \tag{11}$$

where $\tau_2 = i\sigma_2$ (σ_2 is Pauli matrix). The Yukawa interaction of leptons is similar to Eq. (11).

In order to explain the top quark forward-backward asymmetry at Tevatron, we add the new Yukawa interaction:

$$\mathcal{L}_q = \frac{y_u^{\alpha\beta}}{\Lambda}(\bar{Q}_{L\alpha}\tau_2 \hat{H}_L^*)(\hat{H}_R^T \tau_2 Q_{R\beta}) + \frac{y_d^{\alpha\beta}}{\Lambda}(\bar{Q}_{L\alpha} \hat{H}_L)(\hat{H}_R^\dagger Q_{R\beta}) + h.c.. \tag{12}$$

Since the VEV of $\hat{H}_L$ equals to zero, the interaction can not produce the mass term of SM quark. With the mass eigenstates and the expressions of $\hat{H}_L$ and $\hat{H}_R$ shown in [17], we then obtain the following couplings

$$\begin{aligned} \mathcal{L}_q = &- \frac{\hat{f}}{\Lambda}\left(\hat{h}^{0*}\ (X_u)_{\alpha\beta}\ \bar{u}_L^\alpha u_R^\beta - \hat{h}^-\ (V_{CKM}^\dagger X_u)_{\alpha\beta}\ \bar{d}_L^\alpha u_R^\beta\right) \\ &- \frac{\hat{f}}{\Lambda}\left(\hat{h}^0\ (X_d)_{\alpha\beta}\ \bar{d}_L^\alpha d_R^\beta + \hat{h}^+\ (V_{CKM} X_d)_{\alpha\beta}\ \bar{u}_L^\alpha d_R^\beta\right) + h.c.. \end{aligned} \tag{13}$$

To satisfy the constraints from the flavor processes and electroweak data, we take two cases for the mixing matrixes X_u and X_d (the detailed analysis was given in [11]):

(i) Case I: $(X_u)_{\alpha 1} = \kappa_1 (V_{CKM})_{\alpha 3}$, $(X_u)_{\alpha 2} = 0$, $(X_u)_{\alpha 3} = 0$ and $(X_d)_{\alpha\beta} = 0$. From Eq. (13), we can obtain the coupling

$$\begin{aligned} \mathcal{L}_q &= -\frac{\kappa_1 \hat{f}}{\Lambda}\left((V_{CKM})_{\alpha 3}\ \hat{h}^{0*}\ \bar{u}_L^\alpha u_R - \hat{h}^-\ \bar{b}_L u_R\right) + h.c. \\ &= -2y_1\left((V_{CKM})_{\alpha 3}\ \hat{h}^{0*}\ \bar{u}_L^\alpha u_R - \hat{h}^-\ \bar{b}_L u_R\right) + h.c. \end{aligned} \tag{14}$$

with $y_1 = \frac{\kappa_1 \hat{f}}{2\Lambda}$.

(ii) Case II: $(X_u)_{\alpha\beta} = 0$ and $(X_d)_{\alpha\beta} = 0$ except for $(X_d)_{31} = \kappa_2$. From Eq. (13), we can obtain the coupling

$$
\begin{aligned}
\mathcal{L}_q &= -\frac{\kappa_2 \hat{f}}{\Lambda}\left(\hat{h}^0\ \bar{b}_L d_R + (V_{CKM})_{\alpha 3}\ \hat{h}^+\ \bar{u}_L^\alpha d_R\right) + h.c. \\
&= -2y_2\left(\hat{h}^0\ \bar{b}_L d_R + (V_{CKM})_{\alpha 3}\ \hat{h}^+\ \bar{u}_L^\alpha d_R\right) + h.c. \qquad (15)
\end{aligned}
$$

with $y_2 = \frac{\kappa_2 \hat{f}}{2\Lambda}$.

The cut-off scale Λ is typically taken to be $4\pi f$ with f being as low as 500 GeV. Sometime $\Lambda = 2\pi f$ is also considered [17]. The scale $\hat{f}$ can be determined from the electroweak symmetry breaking condition. At a rough estimate, $\hat{f}$ is five times as f or more [17, 29]. For Case I (Case II), $\hat{S}$ and $\hat{A}$ from $\hat{h}^0 = \frac{\hat{S}+i\hat{A}}{\sqrt{2}}$ ($\hat{h}^\pm$) can contribute to the top quark forward-backward asymmetry at the Tevatron via the t-channel exchange of such a scalar. This also implies that $\hat{S}$ or $\hat{A}$ can no longer be the candidate for the WIMP dark matter.

The Coleman-Weinberg potential and the soft left-right symmetry breaking terms (the so-called μ-term) can give masses for $\hat{h}^\pm$ and $\hat{h}^0$ as [17]

$$
\begin{aligned}
m_{\hat{S}}^2 = m_{\hat{A}}^2 = m_{\hat{h}^0}^2 = \frac{3}{16\pi^2}\Big[&\frac{g_2^2}{2}(\mathcal{Z}(m_W) - \mathcal{Z}(m_{W_H})) \\
&+ \frac{2g_1^2 + g_2^2}{4}\frac{m_{W_H}^2 - m_W^2}{m_{Z_H}^2 - m_Z^2}(\mathcal{Z}(m_Z) - \mathcal{Z}(m_{Z_H}))\Big] + \mu_r^2 \frac{f}{\hat{f}}\cos x + \hat{\mu}^2, \qquad (16) \\
m_{\hat{h}^\pm}^2 \simeq m_{\hat{h}^0}^2, \qquad (17)
\end{aligned}
$$

where $\mathcal{Z}(x) = -x^2(\ln\frac{\Lambda^2}{x^2} + 1)$. The last two terms are from the μ-term. We neglect the small mass splitting between $\hat{h}^0$ and $\hat{h}^\pm$ due to the electromagnetic interactions. Note that $\hat{\mu}^2$ could have either sign, which can allow us to vary the masses of $\hat{h}^0$ and $\hat{h}^\pm$ as a free parameter.

Note that, due to an additional phase factor i in the Yukawa coupling of $\hat{A}$, the contributions of $\hat{S}$ and $\hat{A}$ to the same-sign top pair productions are destructive and such contributions can be even canceled for the degeneracy masses of $\hat{S}$ and $\hat{A}$. Thus, the LRTH with such new Yukawa interaction can be free from the strong constraints from tt production rate reported by CMS collaboration, $\sigma(tt) < 17$ pb at 95% C. L. [30].

In fact, we still can introduce a parity in the model under which $\hat{H}$ is odd while all the other fields are even. The non-renormalizable interaction of Eq. (12) is invariant under this parity. This parity can forbid the renormalizable interaction between $\hat{H}$ and fermions,

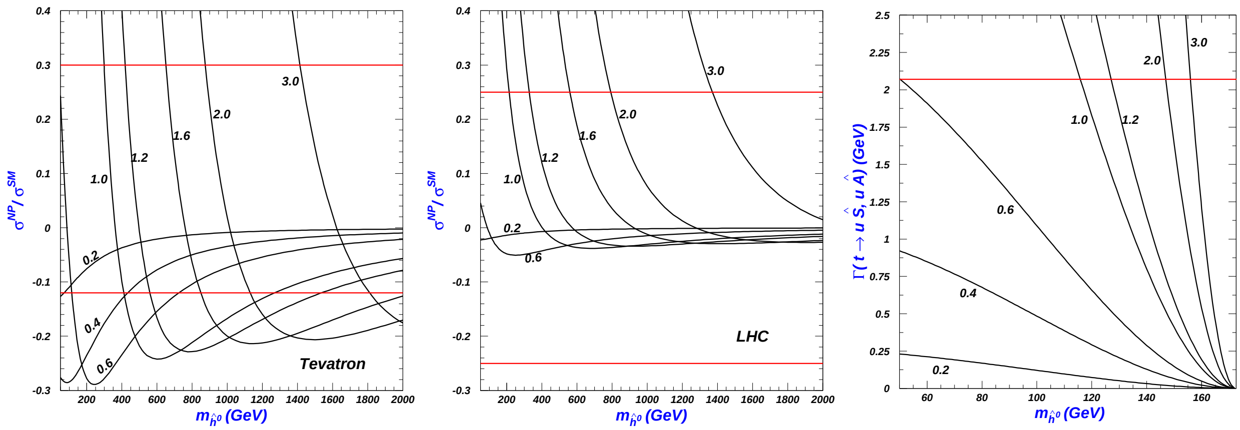

FIG. 1: For Case I, the new physics contributions to $t\bar{t}$ production rates (normalized to SM values) and the decay width of $t \to u\hat{S},\ u\hat{A}$ versus $m_{\hat{h}^0}$. The numbers on the curves denote the Yukawa coupling y_1. The horizontal lines show the 2σ limits from the corresponding experimental data.

especially the top quark. The top quark mass can still be obtained from the renormalizable interaction shown in the original LRTH [17].

III. CALCULATIONS AND DISCUSSIONS

In our calculations, we take $m_t = 172.5$ GeV and use the parton distribution function CTEQ6L [31] with renormalization scale and factorization scale $\mu_R = \mu_F = m_t$. We assume that the K-factors are universal, so that the QCD correction effects are canceled in the ratios of σ^{NP}/σ^{SM} and $\sigma^{NP}/(\sigma^{SM}+\sigma^{NP})$, and they are the same at LO and NLO.

A. Case I: $\hat{S}$ and $\hat{A}$

For Case I, the matrix elements M of the process $u(p_1)\bar{u}(p_2) \to t(k_1)\bar{t}(k_2)$, including the SM, new scalar $\hat{S}$ and $\hat{A}$ contributions, can be written as ref. [12]

$$\sum |M|^2 = \frac{16g_s^4}{s^2}(t_t^2 + u_t^2 + 2sm_t^2) + 32g_s^2y^2\frac{sm_t^2 + t_t^2}{st_{\hat{h}^0}} + 36\frac{y^4t_t^2}{t_{\hat{h}^0}^2}, \tag{18}$$

where $s = (p_1+p_2)^2$, $t = (p_1-k_1)^2$, $u = (p_1-k_2)^2$, $t_t = t - m_t^2$, $t_{\hat{h}^0} = t - m_{\hat{h}^0}^2$, $y = \sqrt{2}y_1$.

In Fig. 1, we plot respectively the new physics contributions to $t\bar{t}$ production at Tevatron and LHC normalized to SM one, and the decay width of $t \to u\hat{S},\ u\hat{A}$ for Case I. We can find that the contributions of $\hat{S}$ and $\hat{A}$ to the $t\bar{t}$ cross section can be positive or negative,

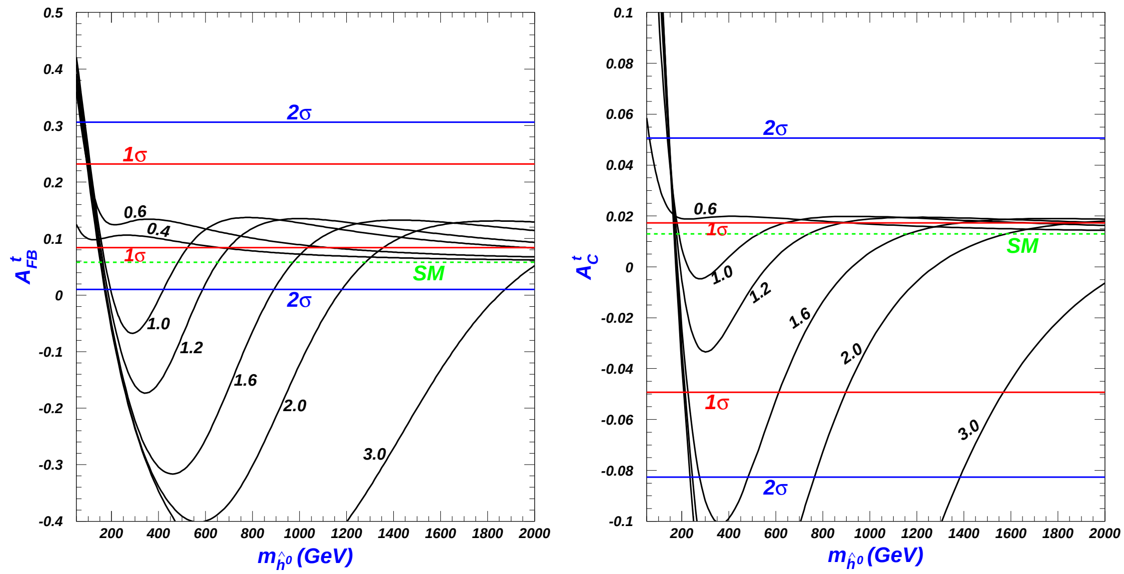

FIG. 2: For Case I, the top forward-backward asymmetry A^t_{FB} at Tevatron and charge asymmetry A^t_C at LHC versus $m_{\hat{h}^0}$. The dash lines denote the SM predictions. The horizontal lines show the 1σ and 2σ ranges from the corresponding experimental data.

which depends on the coupling constant y_1 and their masses. Since the process $gg \to t\bar{t}$ dominates the $t\bar{t}$ cross section at LHC and the contributions of $\hat{S}$ and $\hat{A}$ are from the process $u\bar{u} \to t\bar{t}$, the magnitude of $\frac{\sigma^{NP}}{\sigma^{SM}}$ at LHC is smaller than that of Tevatron. The $t\bar{t}$ cross section measured at Tevatron gives the most constraint on the parameters y_1 and $m_{\hat{h}^0}$. For example, the measurement value requires $m_{\hat{h}^0}$ to be larger than 1200 GeV (2000 GeV) in addition to the narrow intermediate region for $y_1 = 1.0$ (1.6). The $t\bar{t}$ cross section measured at LHC and top quark decay can hardly give further constraints.

In Fig. 2, we plot the top quark forward-backward asymmetry A^t_{FB} at Tevatron and charge asymmetry A^t_C at LHC for Case I. We can see that A^t_{FB} can be enhanced sizably for the very low values of $m_{\hat{h}^0}$, be over 0.1 for the large ones and be negative in the intermediate region. For the large region of $m_{\hat{h}^0}$, the left panel of Fig. 1 shows that $\frac{\sigma^{NP}}{\sigma^{SM}}$ is negative, which can play a positive role in enhancing the A^t_{FB} according to its definition shown in Eq. (1) and Eq. (3). The dependence of A^t_C on y_1 and $m_{\hat{h}^0}$ is similar to that of A^t_{FB}, which is within 1σ range in the large parameter spaces.

In Fig. 3, we scan the following parameter space,

$$0.1 \leq y_1 \leq 1.0, \quad 100\ GeV \leq m_{\hat{h}^0} \leq 2000\ GeV,$$

and plot A^t_{FB} versus A^t_C under the constraints of the three observables shown in Fig. 1. We

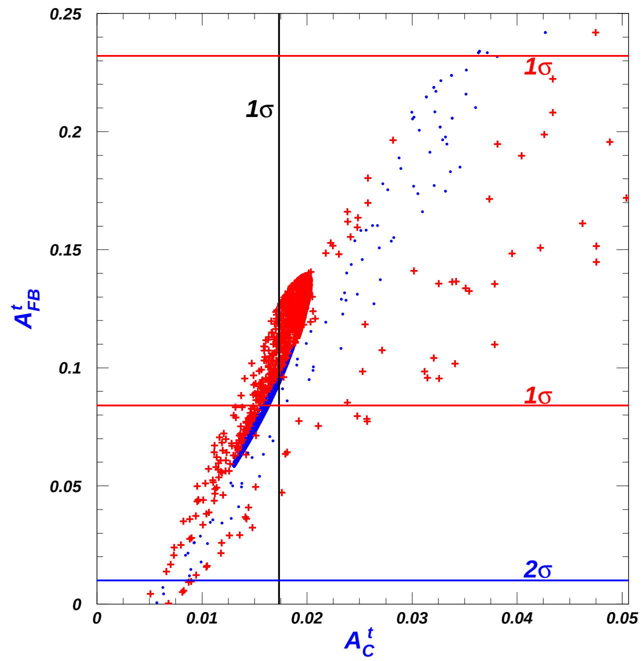

FIG. 3: For Case I, the top quark forward-backward asymmetry A^t_{FB} at Tevatron versus charge asymmetry A^t_C at LHC. The bullets (blue) and crosses (red) are respectively allowed and excluded by the three observables shown in Fig. 1. The horizontal lines show the 1σ and 2σ lower limits from the experimental data of A^t_{FB} at Tevatron. The vertical line shows the 1σ upper limit from the experimental data of A^t_C at LHC.

find that A^t_{FB} and A^t_C have direct correlation, and the former always increases as increasing of the latter. The A^t_{FB} can be explained to within 1σ and reach 0.1 for A^t_C remains within 1σ. For A^t_C is in the range of 1σ and 2σ, A^t_{FB} can reach 0.24. If the future more precision measurement at LHC shows that A^t_C is smaller than 0.0125, the model will lose its spirit of producing a large A^t_{FB} at the Tevatron.

B. Case II: $\hat{h}^{\pm}$

For Case II, the matrix elements M of the process $d(p_1)\bar{d}(p_2) \to t(k_1)\bar{t}(k_2)$, including the SM and $\hat{h}^+$ contributions, is the same as Eq. (18), but replacing $m_{\hat{h}^0}$ and y_1 with $m_{\hat{h}^+}$ and y_2.

In Fig. 4, we plot respectively the new physics contributions to $t\bar{t}$ production at Tevatron and LHC normalized to SM one, and the decay width of $t \to d\hat{h}^+$ for Case II. Compared to Case I, the magnitude of $\frac{\sigma^{NP}}{\sigma^{SM}}$ at Tevatron and LHC for Case II is less sizable due to the

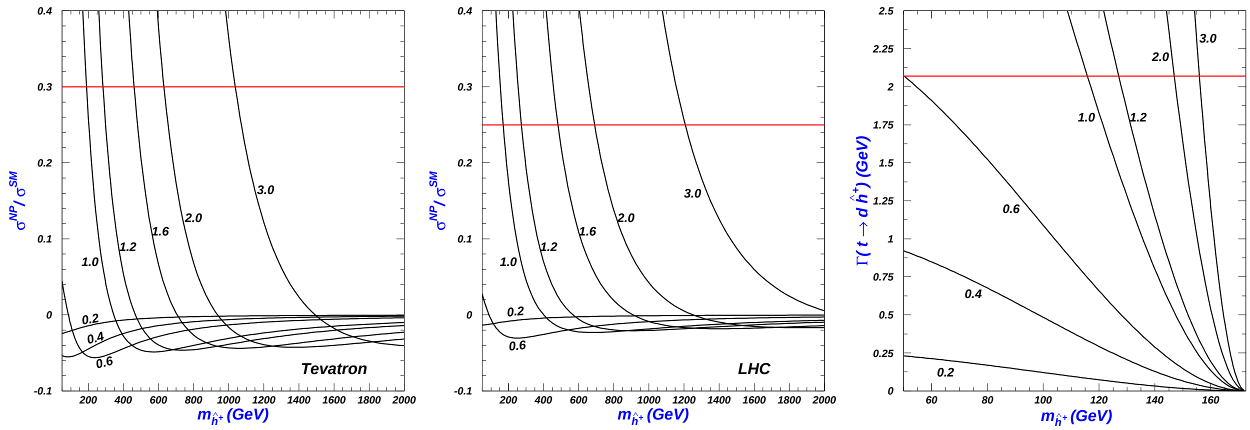

FIG. 4: For Case II, the new physics contributions to $t\bar{t}$ production rates (normalized to SM values) and the decay width of $t \to d\hat{h}^+$ versus $m_{\hat{h}^+}$. The numbers on the curves denote the Yukawa coupling y_2. The horizontal lines show the 2σ upper limits from the corresponding experimental data.

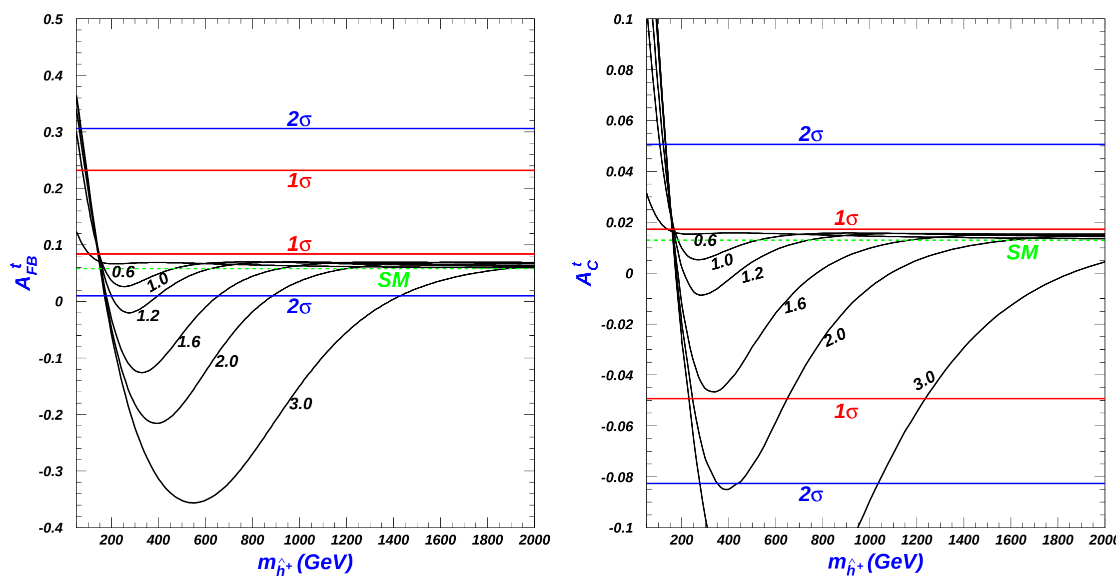

FIG. 5: Same as Fig.2, but for Case II.

smaller parton distribution function of d quark. Therefore, the more broad region of the parameter space for Case II is allowed by the related experimental data of top quark. For example, $m_{\hat{h}^+}$ is required to be larger than 180 GeV (450 GeV) for $y_2 = 1.0$ (1.6).

In Fig. 5, we plot the top quark forward-backward asymmetry A^t_{FB} at Tevatron and charge asymmetry A^t_C at LHC for Case II. The A^t_{FB} can be enhanced sizably for the very low values of $m_{\hat{h}^+}$, be negative in the intermediate region and be outside the range of 1σ for the large ones which differs from the Case I. The A^t_C can be still within 1σ in the most of parameter spaces.

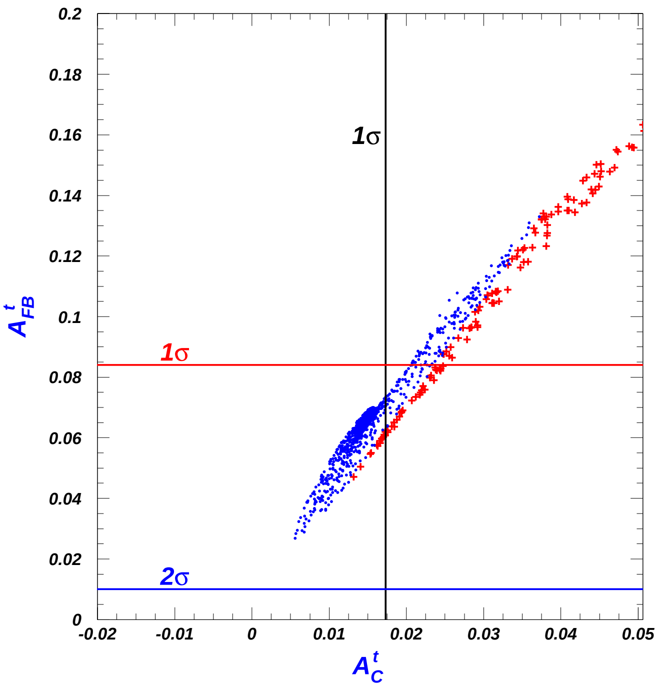

FIG. 6: Same as Fig.3, but for Case II

In Fig. 6, we scan the following parameter space,

$$0.1 \leq y_2 \leq 1.0, \quad 100\ GeV \leq m_{\hat{h}^+} \leq 1000\ GeV,$$

and plot A^t_{FB} versus A^t_C under the constraints of the three observables shown in Fig. 4. We find that the relative large parameter space scanned is allowed by the three experimental data of top quark. The A^t_{FB} is outside the range of 1σ for A^t_C is within 1σ, and reaches 0.13 for A^t_C equals to 0.035 (at 1.5σ). The measurement of A^t_{FB} at Tevatron is complementary to A^t_C at LHC.

C. Other discussions

The $t\bar{t}$ invariant mass distribution was measured by CDF, and the results are presented in nine bins of $M_{t\bar{t}}$ [32], which does not give enough solid constraint on this model since the QCD correction and cut efficiency may significantly modify the shape of differential distribution $d\sigma/d_{M_{t\bar{t}}}$ [7, 8, 33]. However, we will further examine the constraints of the invariant mass distribution by requiring the differential cross section in each bin to be within the 2σ regions of their experimental values. We scan the y_1 (y_2) and $m_{\hat{h}^0}$ ($m_{\hat{h}^+}$) in the region where the total width of top quark, $t\bar{t}$ production cross sections at Tevatron and LHC are in agreement

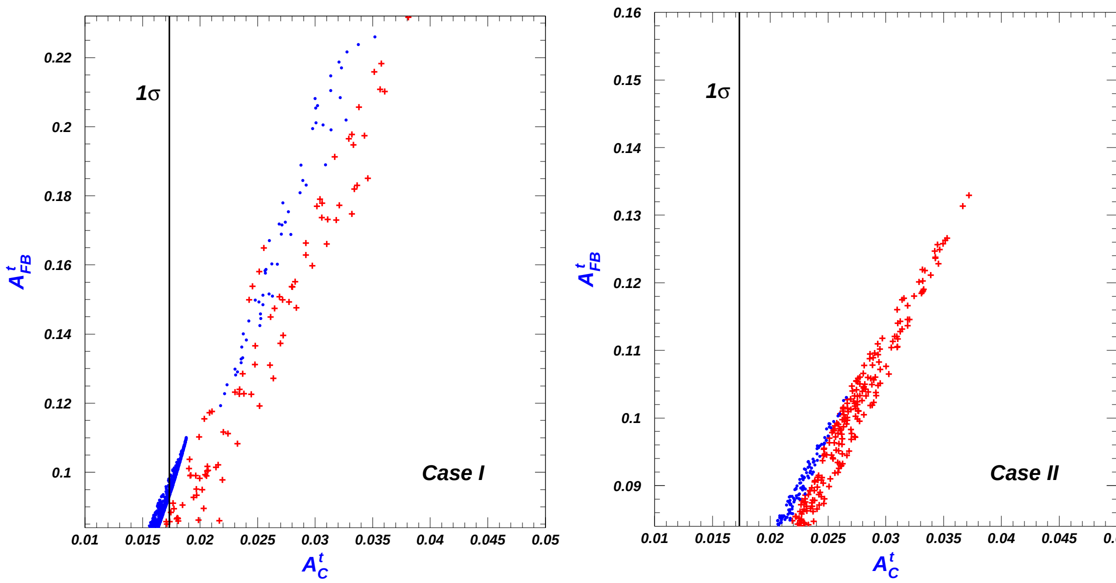

FIG. 7: Top quark forward-backward asymmetry A^t_{FB} at Tevatron versus charge asymmetry A^t_C at LHC. All the plots are in agreement with the constraints from the total width of top quark, $t\bar{t}$ production cross sections at Tevatron and LHC. The bullets (blue) and crosses (red) are respectively allowed and excluded by the experimental data of the $t\bar{t}$ invariant mass distribution at Tevatron.

with the corresponding constraints of experimental data. We plot respectively A^t_{FB} versus A^t_C for Case I and Case II in Fig. 7, where A^t_{FB} is within 1σ range of the experimental value. From Fig. 7, we can find that the constraints of $t\bar{t}$ invariant mass distribution can further exclude some values of A^t_{FB} and A^t_C. For Case I, our previous conclusions are not changed. For Case II, some large values of A^t_{FB} are disfavored by the constraints of invariant mass distribution.

The values of y_1 (y_2) and $m_{\hat{h}^0}$ ($m_{\hat{h}^+}$) corresponding to Fig. 7 are shown in Fig. 8. When $0.6 \leq y_1 \leq 0.7$ ($0.6 \leq y_2 \leq 0.75$) and 100 GeV $< m_{\hat{h}^0} <$ 200 GeV (100 GeV$< m_{\hat{h}^+} <$ 140 GeV), A^t_{FB} is allowed to be within the $+1\sigma$ (-1σ) range for Case I (Case II). In such parameter space, this model can fit best the experimental data of A^t_{FB}. When $y_1(y_2) = 0.6$, $\kappa_1(\kappa_2)$ should be around 1.5 for $\Lambda = 2\pi f$ and 3.0 for $\Lambda = 4\pi f$ taking $\hat{f} = 5f$ (see Eqs. (14) and (15)). Thus, an unnaturally large $\kappa_1(\kappa_2)$ is not necessary for A^t_{FB} is within 1σ range.

For Case I, $\hat{S}$ ($\hat{A}$) can decay into an up quark and an up-type quark. For Case II, $\hat{h}^{\pm}$ can decay into a down quark and an up-type quark. Except for the decay into top quark, the other decays will be suppressed by the corresponding mixing matrix element. For masses of these scalars are much larger than top quark mass, their total widths can reach the half of

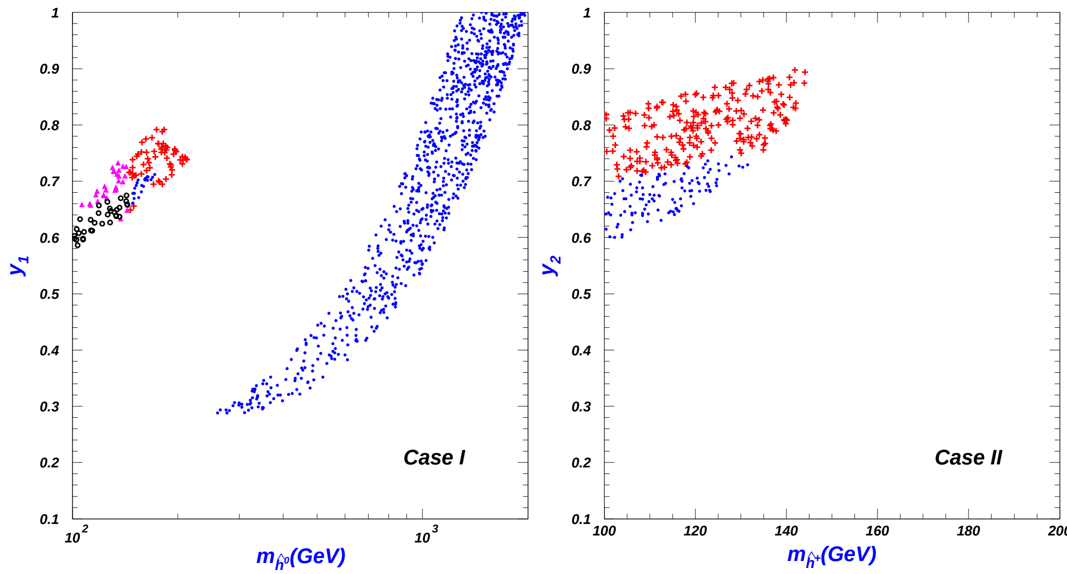

FIG. 8: y_1 (y_2) and $m_{\hat{h}^0}$ ($m_{\hat{h}^+}$) corresponding to Fig. 7. For the bullets (blue) and crosses (red), A^t_{FB} is within -1σ range; For the circles (black) and triangle (pink), A^t_{FB} is within +1σ range. The circles (black) and bullets (blue) are allowed by the experimental data of the $t\bar{t}$ invariant mass distribution at Tevatron; The crosses (red) and triangle (pink) are excluded by this data.

the masses taking $y_1 = y_2 = 1$, respectively. We find that the value of A^t_{FB} is not changed sizably when varying the width from zero GeV to the half of scalar mass, especially for that A^t_{FB} is within +1σ range for Case I and within 1σ range for Case II. The reason is that the widths of these scalars are very small for such values of A^t_{FB}, which can be derived according to the parameters shown in Fig. 8.

The D0 has recently measured single top quark production cross section at Tevatron by requiring one b-jet in the final states and obtained $\sigma(p\bar{p} \to tqb + X) = 2.90 \pm 0.59$ pb [34], where q is a light quark. The experimental value is in agreement with the SM t-channel tbq result of 2.26 ± 0.12 pb. For Case I and Case II, the single top can be produced by the process $gu \to t\hat{S}$ ($\hat{A}$) and $gd \to t\hat{h}^-$, respectively. In Fig. 9, we plot the A^t_{FB} versus the cross sections of the single top quark associated with the scalar production at Tevatron for Case I and Case II. We find that the cross sections can be over 1 pb when A^t_{FB} is larger than 0.15 for Case I and 0.1 for Case II, respectively. However, given that $\hat{S}$, $\hat{A}$ and $\hat{h}^\pm$ can not decay into a bottom quark, this constraint is not suitable for our model due to the lack of b-jet in the final states. A dedicated study is required in order to establish the applicability of the single top measurements at the Tevatron to our model.

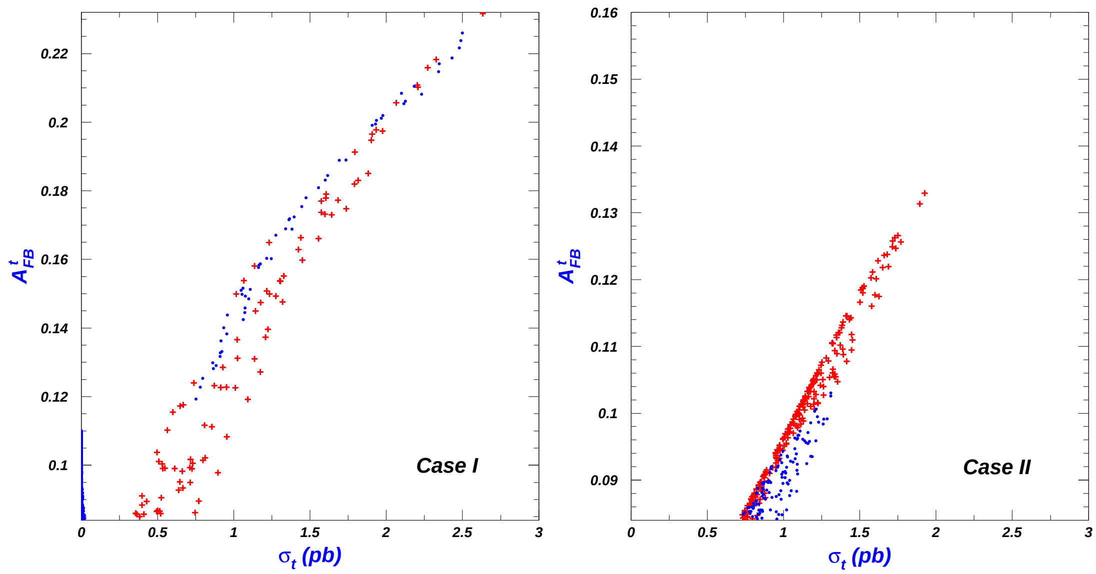

FIG. 9: Same as Fig. 7, but for A^t_{FB} versus σ_t. σ_t denotes the cross section of the single top quark associated with the scalar production at Tevatron. $\sigma_t \equiv \sigma\left(gu \to t\hat{S}(\hat{A})\right) + \sigma\left(g\bar{u} \to \bar{t}\hat{S}(\hat{A})\right)$ for Case I; $\sigma_t \equiv \sigma\left(gd \to t\hat{h}^-\right) + \sigma\left(g\bar{d} \to \bar{t}\hat{h}^+\right)$ for Case II.

In the LRTH model, there exist additional heavy gauge bosons from the $SU(2)_R$ symmetric sector, dubbed $W_H^\pm$ and Z_H, which can also contribute to the top quark forward-backward asymmetry. In this model, the $SU(2)_{L,R}$ coupling constants g_L and g_R are identical. The experimental limits favor that the quark mixing matrices in the left- and right-handed sectors are the same [17]. For this case, Ref. [9] shows that the value of A^t_{FB} produced by $W_H^\pm$ and Z_H is much smaller than the experimental value. Compared with the contributions of $\hat{h}^\pm$, $\hat{S}$ and $\hat{A}$, their contributions can be ignored safely.

IV. CONCLUSION

In the framework of left-right twin Higgs model we introduced a new Yukawa interaction for the doublet $\hat{h}$, which leads that the lightest neutral particle of $\hat{h}$ can no longer be the dark matter candidate. Such new Yukawa interaction was found to sizably contribute to the top quark forward-backward asymmetry A^t_{FB} at the Tevatron. Under the constraints from the related experimental data of top quark, we found that the Tevatron A^t_{FB} can be explained while the LHC charge asymmetry A^t_C measurement can also be satisfied.

Although explaining A^t_{FB} by extending Higgs sector has been studied in some papers, most of them do not propose a realistic model. By introducing the new Yukawa interaction,

we make the LRTH to be a realistic one, which can solve the hierarchy problem in addition to A^t_{FB}. Besides, the degeneracy masses of $\hat{S}$ and $\hat{A}$ can naturally avoid the strong constraints of the same-sign top pair production at LHC, leading A^t_{FB} to reach 0.24.

Acknowledgment

We thank Manuel Perez-Victoria for helpful comment. This work was supported in part by the National Natural Science Foundation of China (NNSFC) under grant Nos. 11105116 and 11005089, 10725526, 10821504 and 10635030, and by the Project of Knowledge Innovation Program (PKIP) of Chinese Academy of Sciences under grant No. KJCX2.YW.W10.

---

[1] CDF Collaboration, Phys. Rev. D **83**, 112003 (2011).

[2] D0 Collaboration, Phys. Rev. D **84**, 112005 (2011).

[3] J. H. Kuhn and G. Rodrigo, Phys. Rev. Lett. **81**, 49 (1998); J. H. Kuhn and G. Rodrigo, Phys. Rev. D **59**, 054017 (1999); M. T. Bowen, S. D. Ellis and D. Rainwater, Phys. Rev. D **73**, 014008 (2006); O. Antunano, J. H. Kuhn and G. Rodrigo, Phys. Rev. D **77**, 014003 (2008).

[4] V. Ahrens, A. Ferroglia, M. Neubert, B. D. Pecjak, L. L. Yang, Phys. Rev. D **84**, 074004 (2011).

[5] P. Ferrario, G. Rodrigo, Phys. Rev. D **80**, 051701 (2009); P. Ferrario and G. Rodrigo, JHEP **1002**, 051 (2010); P. H. Frampton *et al.*, Phys. Rev. D **683**, 294 (2010); M. V. Martynov, A. D. Smirnov, Mod. Phys. Lett. A **25**, 2637 (2010); R. S. Chivukula *et al.*, Phys. Rev. D **82**, 094009 (2010); Y. Bai *et al.*, JHEP **1103**, 003 (2011); A. Djouadi *et al.*, Phys. Rev. D **82**, 071702 (2010); K. Kumar *et al.*, JHEP **1008**, 052 (2010); G. Burdman *et al.*, Phys. Rev. D **83**, 035012 (2011); E. Alvarez *et al.*, JHEP **1105**, 070 (2011); C. Delaunay *et al.*, arXiv:1101.2902; M. Bauer *et al.*, JHEP 1011, 039 (2010); C. H. Chen *et al.*, Phys. Lett. B **694**, 393 (2011); R. Foot, Phys. Rev. D **83**, 114013 (2011); A. Djouadi *et al.*, Phys. Lett. B **701**, 458 (2011); R. Barcelo *et al.*, arXiv:1105.3333; G. M. Tavares and M. Schmaltz, arXiv:1107.0978; E. Alvarez *et al.*, arXiv:1107.1473; E. Gabrielli, M. Raidal, arXiv:1106.4553; H. Wang *et al.*, arXiv:1107.5769; G. Z. Krnjaic, arXiv:1109.0648; H. Davoudiasl, T. McElmurry, A. Soni,

arXiv:1108.1173; E. L. Berger *et al.*, arXiv:1111.3641; X.-P. Wang et al., Phys. Rev. D **83**, 115010 (2011); J. A. Aguilar-Saavedra, M. Perez-Victoria, Phys. Lett. B **705**, 228-234 (2011).

[6] K. Cheung *et al.*, Phys. Lett. B **682**, 287 (2009); S. Jung, *et al.*, Phys. Rev. D **81**, 015004 (2010); V. Barger *et al.*, Phys. Rev. D **81**, 113009 (2010); I. Dorsner *et al.*, Phys. Rev. D **81**, 055009 (2010); A. Arhrib, R. Benbrik, C. H. Chen, Phys. Rev. D **82**, 034034 (2010); G. Rodrigo, P. Ferrario, Nuovo Cim. C **33**, 04 (2010); J. Cao *et al.*, Phys. Rev. D **81**, 014016 (2010); Phys. Rev. D **83**, 034024 (2011); Phys. Rev. D **84**, 074001 (2011); arXiv:1109.6543; S. Jung, A. Pierce, J. D. Wells, Phys. Rev. D **83**, 114039 (2011); B. Bhattacherjee *et al.*, Phys. Rev. D **83**, 091501 (2011); K. M. Patel, P. Sharma, JHEP **1104**, 085 (2011); M. R. Buckley, *et al.*, Phys. Rev. D **83**, 115013 (2011); G. Isidori and J. F. Kamenik, Phys. Lett. B **700**, 145 (2011); E. R. Barreto *et al.*, Phys. Rev. D **83**, 054006 (2011); A. Rajaraman, Z. E. Surujon, T. M. P. Tait, arXiv:1104.0947; M. I. Gresham *et al.*, arXiv:1107.4364; Y. Cui *et al.*, arXiv:1106.3086; M. Duraisamy, A. Rashed, A. Datta, arXiv:1106.5982; B. Grinstein, *et al.*, arXiv:1108.4027; D. Kahawala, D. Krohn, M. J. Strassler, arXiv:1108.3301; P. Ko, Y. Omura, C. Yu, arXiv:1108.4005; S. K. Gupta, arXiv:1011.4960; E. L. Berger *et al.*, Phys. Rev. Lett. **106**, 201801 (2011); arXiv:1109.3202; K. Cheung and T. C. Yuan, Phys. Rev. D **83**, 074006 (2011); Z. Ligeti, G. M. Tavares, M. Schmaltz, JHEP **1106**, 109 (2011). M. I. Gresham, I. W. Kim, K. M. Zurek, Phys. Rev. D **83**, 114027 (2011); J. F. Kamenik, J. Shu, J. Zupan, arXiv:1107.5257; S. Westhoff, arXiv:1108.3341; K. Yan *et al.*, arXiv:1110.6684.

[7] J. Shu, K. Wang, G. Zhu, Phys. Rev. D **85**, 034008 (2012).

[8] B. Xiao, Y.-k. Wang, S. -h. Zhu, Phys. Rev. D **82**, 034026 (2010).

[9] M. Frank, A. Hayreter, I. Turan, Phys. Rev. D **84**, 114007 (2011).

[10] Q.-H. Cao *et al.*, Phys. Rev. D **81**, 114004 (2010).

[11] K. Blum, Y. Hochberg, Y. Nir, JHEP **1110**, 124 (2011).

[12] J. Shu, T. M. P. Tait, K. Wang, Phys. Rev. D **81**, 034012 (2010).

[13] D. W. Jung *et al.*, Phys. Lett. B **691**, 238 (2010); arXiv:1012.0102; C. Zhang, S. Willenbrock, arXiv:1008.3869; J. A. Aguilar-Saavedra, Nucl. Phys. B **843**, 638 (2011); Nucl. Phys. B **812**, 181 (2009); C. Degrande *et al.*, arXiv:1010.6304; K. Blum *et al.*, arXiv:1102.3133; C. Delaunay *et al.*, arXiv:1103.2297; C. Degrande *et al.*, arXiv:1104.1798; D. Y. Shao *et al.*, arXiv:1107.4012; J. A. Aguilar-Saavedra, M. Perez-Victoria, Phys. Lett. B **701**, 93 (2011); JHEP **1105**, 034 (2011).

[14] J. A. Aguilar-Saavedra, M. Perez-Victoria, JHEP **1109**, 097 (2011).

[15] Z. Chacko, H. S. Goh, and R. Harnik, Phys. Rev. Lett. **96**, 231802 (2006); R. Barbieri, T. Gregoire, and L. J. Hall, hep-ph/0509242; Z. Chacko, Y. Nomura, M. Papucci, G. Perez, JHEP **01**, 126 (2006); R. Foot, R. R. Volkas, Phys. Lett. B **645**, 75 (2007); A. Falkowski, S. Pokorski, M. Schmaltz, Phys. Rev. D **74**, 035003 (2006); S. Chang, L. J. Hall, N. Weiner, Phys. Rev. D **75**, 035009 (2007).

[16] Z. Chacko, H. S. Goh, R. Harnik, JHEP **0601**, 108 (2006).

[17] H. S. Goh, S. Su, Phys. Rev. D **75**, 075010 (2007).

[18] E. M. Dolle, S. Su, Phys. Rev. D **77**, 075013 (2008); L. Wang, J. M. Yang, JHEP **1005**, 024 (2010).

[19] J. L. Hewett *et al.*, Phys. Rev. D **84**, 054005 (2011); J. F. Arguin, M. Freytsis and Z. Ligeti, Phys. Rev. D **84**, 071504 (2011).

[20] http://cdsweb.cern.ch/record/1369205/files/TOP-11-014-pas.

[21] http://cdsweb.cern.ch/record/1372916/files/ATLAS-CONF-2011-106.

[22] T. Aaltonen et al. [CDF Collaboration], CDF note 9913.

[23] U. Langenfeld, S. Moch, P. Uwer, Phys. Rev. D **80**, 054009 (2009).

[24] V. Ahrens, et al., JHEP **1009**, 097 (2010).

[25] ATLAS Collaboration, arXiv:1110.1027.

[26] CMS Collaboration, JHEP **1107**, 049 (2011).

[27] V. Ahrens et al., JHEP **09**, 097 (2010).

[28] V. M. Abazov et al. [D0 Collaboration], Phys. Rev. Lett. **106**, 022001 (2011).

[29] D.-W. Jung, J. Y. Lee, hep-ph/0701071.

[30] CMS Collaboration, JHEP **1108**, 005 (2011).

[31] J. Pumplin et al., JHEP **0602**, 032 (2006).

[32] CDF Collaboration], Phys. Rev. Lett. **102**, 222003 (2009).

[33] M. I. Gresham, I. -W. Kim, K. M. Zurek, Phys. Rev. D **83**, 114027 (2011).

[34] D0 Collaboration, Phys. Lett. B **705**, 313 (2011).